



## Undergraduate Graduation Thesis

基于 3D 打印的血管流物理实验与数值模拟研究

Physical Experiment and Numerical Simulation of  
Vascular Flow Based on 3D Printing

Department of Engineering

詹玉婷 Yuting Zhan

Supervisor ( Title ) : 詹杰民教授 Prof. Jiemin Zhan

May 11 2017

# Table of Contents

1. Introduction .....	9
1.1 Background .....	9
1.2 Purpose .....	10
1.3 Introduction and Current Development of Relative Filed .....	11
1.3.1 CFD Computational Fluid Dynamics Modeling Analysis .....	11
1.3.2 Finite element method .....	12
1.3.3 Hemodynamics .....	13
1.3.4 Three-Dimensional Printing (3D Printing) .....	13
1.3.5 Overview of ANSYS .....	14
1.4 Main Content .....	15
2. Two Mathematical Techniques and Numerical Analysis .....	17
2.1 Non-Uniform Rational B-spline Surface (NURBS) .....	17
2.2 Governing Equation .....	18
2.2.1 Reynolds number .....	18
2.2.2 Navier-Stoke Equations .....	18
2.3 Tetrahedron and Hexahedron .....	20
3. Three Image Reconstruction and Establishment of Vascular Flow Model .....	21
3.1 3D Reconstruction of the blood flow area --- Boolean Rules .....	21
3.2 Reverse Engineering --- Geomagic Studio 12 .....	21
3.3 Mesh .....	23
3.4 Numerical realization .....	24
4. Experimental Investigation of Blood Vessel Flow in Abdominal Artery .....	25
4.1 Physical Experiment Parameters Setup .....	25
4.2 Experiment Device Design .....	25
4.2.1 Experiment Device Design Method .....	25
4.2.2 Photos of Experiment Device .....	26
4.3 Experiment Results .....	26
5. Numerical Investigation of Blood Vessel Flow in Abdominal Artery .....	27
5.1 Velocity Simulation Results .....	28
5.1.1 Comparison of Velocity Vector Field .....	28
5.1.2 Comparison of Velocity Streamline .....	29
5.2 Pressure Simulation Results .....	30
5.2.1 Comparison of Pressure Vector Field .....	30
5.2.2 Comparison of how Pressure changes inside the fluid zone .....	31
5.2.3 Comparison of Pressure Contour .....	32

5.2.4 Comparison of total pressure at the artery wall .....	33
5.3 Wall Shear Stress Simulation Results .....	34
5.3.1 Comparison of Shear Stress at the Artery wall .....	34
5.3.2 Comparison of Wall Shear stress contour .....	35
6. Validation between Physical Experiment and Numerical Simulation with 0.1m/s inlet velocity .....	36
7. Conclusion and Prospect .....	37

## List of Figures

Figure3. 1 NURBS surface of healthy abdominal artery .....	22
Figure3. 2 NURBS surface of AAA model .....	22
Figure3. 3 Mesh of the healthy Abdomnial Artery model .....	23
Figure3. 4 Mesh of the AAA model .....	23
Figure4. 1 Velocity Vector Distribution of Healthy Abdominal Artery (Specific Orientation) .....	28
Figure4. 2 Velocity Vector Distribution of Abdominal Aneurysm (Specific Orientation) .....	28
Figure4. 3 Velocity Vector Distribution of Healthy Abdominal Artery (Default Orientation) .....	28
Figure4. 4 Velocity Vector Distribution of Abdominal Aneurysm (Default Orientation) .....	28
Figure4. 5 Velocity Streamline of Healthy Abdominal Artery (Specific Orientation) .....	29
Figure4. 6 Velocity Streamline of Abdominal Artery Aneurysm (Specific Orientation) .....	29
Figure4. 7 Velocity Streamline of Healthy Abdominal Artery (Default Orientation) .....	29
Figure4. 8 Velocity Streamline of Abdominal Artery Aneurysm (Default Orientation) .....	29
Figure4. 9 Pressure Vector Distribution of Healthy Abdominal Artery (Specific Orientation) .....	30
Figure4. 10 Pressure Vector Distribution of Abdominal Artery Aneurysm (Specific Orientation) .....	30
Figure4. 11 Pressure Vector Distribution of Healthy Abdominal Artery (Default Orientation) .....	30
Figure4. 12 Pressure Vector Distribution of Abdominal Artery Aneurysm (Default Orientation) .....	30
Figure4. 13 Pressure Distribution of Healthy Abdominal Artery (Specific Orientation) .....	31
Figure4. 14 Pressure Distribution of Abdominal Artery Aneurysm (Specific Orientation) .....	31
Figure4. 15 Pressure Distribution of Healthy Abdominal Artery (Default Orientation) .....	31
Figure4. 16 Pressure Distribution of Abdominal Artery Aneurysm (Default Orientation) .....	31
Figure4. 17 Artery Wall Pressure Contour of Healthy Abdominal Artery (Specific Orientation) .....	32
Figure4. 18 Artery Wall Pressure Contour of Abdominal Aneurysm (Specific Orientation) .....	32
Figure4. 19 Artery Wall Pressure Contour of Healthy Abdominal Artery (Default Orientation) .....	32
Figure4. 20 Artery Wall Pressure Contour of Abdominal Aneurysm (Default Orientation) .....	32
Figure4. 21 Artery Wall Pressure Distribution of Healthy Abdominal Artery (Specific Orientation) .....	33
Figure4. 22 Artery Wall Pressure Distribution of Abdominal Aneurysm (Specific Orientation) .....	33
Figure4. 23 Artery Wall Pressure Distribution of Healthy Abdominal Artery (Default Orientation) .....	33
Figure4. 24 Artery Wall Pressure Distribution of Abdominal Aneurysm (Default Orientation) .....	33
Figure4. 25 Artery Wall Shear Distribution of Healthy Abdominal Artery (Specific Orientation) .....	34
Figure4. 26 Artery Wall Shear Distribution of Abdominal Artery Aneurysm (Specific Orientation) .....	34
Figure4. 27 Artery Wall Shear Distribution of Healthy Abdominal Artery (Default Orientation) .....	34
Figure4. 28 Artery Wall Shear Distribution of Abdominal Artery Aneurysm (Default Orientation) .....	34
Figure4. 29 Artery Wall Shear Contour of Healthy Abdominal Artery (Specific Orientation) .....	35
Figure4. 30 Artery Wall Shear Contour of Abdominal Artery Aneurysm (Specific Orientation) .....	35
Figure4. 31 Artery Wall Shear Contour of Healthy Abdominal Artery (Default Orientation) .....	35
Figure4. 32 Artery Wall Shear Contour of Abdominal Artery Aneurysm (Default Orientation) .....	35
Table 1. Physical Experiment Result .....	36
Table 2. Simulation Result .....	36

## **Abstract**

Based on the knowledge of hemodynamics and related disciplines, this paper uses advanced 3D reconstruction software and finite element analysis software to compare the healthy abdominal aorta and abdominal aortic aneurysm (AAA). Many medical studies have shown that AAA have high mortality and unavoidable disability rates. Therefore, the potential research results can help doctors understand the occurrence of AAA and its rupture mechanism to help people have more understanding of the disease, and early prevention. Factors such as velocity vector, vascular wall force and wall shear stress was studied to predict the effect of these factors on the formation and development of AAA. However, these parameters are not easily measured and analyzed in the human body due to experimental limitations and other unavoidable factors such as costly, cumbersome, high risk and time-assuming. ANSYS can numerically simulate the computer aneurysm blood flow and observe the hemodynamic system that can be used to explore the possible development or rupture mechanism of aneurysms. The arterial blood flow was simulated by ANSYS FLUENT, and the results were displayed and compared using software generated graphs. Through the intuitive image analysis, people can clearly show the speed field, pressure field and stress field of each position. The numerical simulation results are similar to those of the known flow of blood vessels. It can help doctors to the correct assessment of the risk of aneurysms.

In this paper, on the one hand, a printed 3D model is used to measure and calculate inlet and outlet pressures to observe blood flow in physical experiments. On the other hand, ANSYS was used to simulate abdominal arterial flow. And then compare the results between the experimental part and the numerical simulation part to evaluate the accuracy of the ANSYS numerical simulation and thus determine. Simulation and comparison of healthy abdominal arteries and AAA can provide information on how blood flow affects the pathology and rupture mechanisms of AAA and can help physicians design specific treatment regimens for potential patients.

In this paper, the physical experiments using water as a simulated blood, by comparing the left and right exports of the flow ratio, to determine whether the ANSYS numerical simulation is in line with the actual situation. The data show that the error of the physical experiment is within the allowable range, and the similarity between the experiment and the numerical simulation proves that ANSYS has some reference for the numerical simulation of the blood vessel flow, so it can be used to simulate the health model with ANSYS Lesion model in the pressure field, the velocity

field and the wall stress field difference, so as to study these factors for the formation of angioma pathology significance, to the relevant medical field to provide a reliable reference.

This article only from a single model to compare and draw conclusions, the results have a certain reference significance but does not rule out the chance. ANSYS for a small number of models of the calculation, the results are accurate and simple operation. But in order to make the study more meaningful, in the face of large data calculation, the use of ANSYS will become lengthy and time-consuming, so open-source software such as Palabos can make this calculation can greatly improve the calculation speed and accuracy. At the same time, the GPU accelerated lattice Boltzmann method (LBM) is a recommended alternative to the discharge flow simulation, which preserves the model, and with the perfect GPU mathematic parallel structure can be greatly reduced by parallelizing the computation time. 4D MRI speed scanning has recently been developed rapidly, so we can compare the simulation results with the actual flow conditions. In the physical experiment, for the import and export conditions set relatively rough, in the improvement of equipment and measuring instruments under the conditions, you can get more accurate physical simulation data, so as to get a better conclusion.

**Key words: N-S Equations; Fluid Mechanics; AAA; Abdominal Artery; Hemodynamics; Finite Element Analysis; 3D Printing.**

## 【摘要】

本文基于血液动力学和相关学科的知识，采用先进的三维重建软件和有限元分析软件比较健康的腹主动脉和腹主动脉瘤（AAA）。通过三维重建，数值分析和模拟的方法，研究血管中各种因素（如速度矢量，血管壁力，壁剪应力）之间的关系，以预测这些因素对于腹主动脉瘤形成与发展的影响。很多医学研究表明，腹主动脉瘤具有高死亡率和不可避免的残疾率。因此，潜在的研究成果可以帮助医生了解腹主动脉瘤的发生及其破裂机制，帮助人们更多地了解这种疾病，并提前预防。近年来，成千上万的实验和研究表明，血流速度，压力，壁剪切应力等主要动力学参数在动脉瘤病理生理学中具有重要作用。血管壁面切应力是动脉血管发生病变的一个重要因素，也是现代血流动力学的一个重要指标。但由于实验的限制和其他不可避免的因素（如成本高昂，过程繁琐，高风险率和冗长费时），这些参数在人体内不容易测量和分析。ANSYS 可以数值模拟计算机动脉瘤血流，观察血流动力学系统，可用于探索动脉瘤的可能发展或破裂机制。利用 ANSYS FLUENT 模拟了动脉血流，利用软件生成的图形将结果进行展示和比对。通过直观的图像分析，可以清楚地展示各个位置的速度场，压力场和应力场。数值模拟结果与已知的血管流流动情况相似。它可以帮助医生对动脉瘤的风险进行正确的评估。流体（气体和液体）流动由表示质量，动量和能量的守恒定律的偏微分方程决定。人类血液是一种粘性不可压缩流体，通常由流体力学中的速度分散的连续方程（也称为不可压缩方程）和著名的 Navier-Stokes 方程来描述。Navier-Stokes 方程（N-S 方程）是流体运动的控制方程，其基于质量守恒，牛顿第二定律和能量守恒。N-S 方程描述了运动流体的速度，压力，温度和密度如何相关。它们由时间和空间的偏微分导数构成。在本文中，一方面，使用印刷的 3D 模型来测量和计算入口速度和出口压力，以便在物理实验中观察血流。另一方面，使用 ANSYS 来模拟腹部动脉血管流动。然后比较实验部分和数值模拟部分之间的结果以评估 ANSYS 数值模拟的准确性，从而决定。健康腹部动脉和腹主动脉瘤的模拟和比较可以提供血流如何影响 AAA 的病理和破裂机制的信息，可以帮助医生为潜在患者设计具体的治疗方案。

为了对比研究健康腹部动脉和动脉瘤不同的速度场和压力场，同时比对相应的 3D 模型在物理实验中所得出的数据，从而分析动脉瘤的形成和破裂机制。本文的物理实验采用了水作为模拟血液，两者具有相似的密度和性质，通过对比左右两个出口的流量比，从而判断 ANSYS 数值模拟是否符合实际情况。通过 3D 打印技术打印出来的血管模型与储水器 and 出口处的量筒相连，模拟了一样的血管环境，通过高频相机记录同一时间内两个出口分别的流量，计算其流量比并与 ANSYS 数值模拟的流量比进行比对。数据表明，物理实验的误差在允许的范围内，且实验与数值模拟的相似性证明了 ANSYS 对于血管流的数值模拟具有一定的参考性，因此可以用 ANSYS 数值模拟去直观地比对健康模型与病变模型在压力场，速度场和壁面应力场的差别，从而研究这些因素对于血管瘤病理形成的意义，给相关医学领域提供可靠的参考依据。

本文仅从单个的模型进行比对并得出结论，其结果具有一定的参考意义但是也不排除偶然性。ANSYS 对于少量模型的计算，结果精确并操作简单。但是为了使研究更具参考意义，在面对大数据计算时，ANSYS 的使用则会变得冗长且费时，因此以 Palabos 等开源软件可以对这种计算可以大大地提高计算速度和精度。同时，GPU 加速格子波尔兹曼方法（LBM）是排出流模拟的推荐替代方法，该方法保留了模型，

且与完美的 GPU 数学并行结构可以通过并行化大大缩短计算时间。4D MRI 速度扫描近来得到快速发展，因此我们可以将仿真结果与实际流量条件进行比较。在物理实验方面，对于进出口条件设置比较粗糙，在改进设备和测量仪器的条件下，可以得到更加精确地物理模拟数据，从而得到更好的结论。

**【关键词】：** N-S 方程；流动机理；AAA；腹部动脉；血液动力学；有限元分析；3D 打印。



# 1. Introduction

## 1.1 Background

Fundamental fluid mechanics, which are important for the understanding of the blood flow in the cardiovascular circulatory system of the human body aspects are presented.

Aneurysm, also known as an arteriovenous tumor, refers to the vascular wall local tumidness, similar to the balloon filled with blood swelling. Aneurysms with high lethality and it will appear in any blood vessels, such as the Circle of Willis in the brain, thoracic aortic aneurysm, and abdominal aortic aneurysm [1, 2].

When the aneurysm volume becomes larger, the risk of rupture also increased. Aneurysm rupture can cause bleeding. An aneurysm is a result of weakening the vessel wall, which may be genetic disease or an acquired disease [3]. Aneurysm site may also cause thrombosis and embolism.

Abdominal Aortic Aneurysm (AAA), which is a localized and tumor-like bulge of the abdominal aorta (when the diameter greater than 3cm or more than 50% of the normal diameter) [4], is one kind of the most common aneurysm. The pathogenesis of AAA is due to localized atherosclerosis or trauma of the abdominal aortic wall, especially in the endometrial destruction, which results in weakening abdominal aortic wall and localized-diffusional expansion. Aneurysm dilation and rupture are due by the decline of the vascular smooth muscle elastin along with the increasing ages, and the inefficiency of the collagen safety net failure [5].

The mortality of the AAA patients is four times of the normal person. Most of the AAA occur after 50-year olds, especially for the males and those persons with family history. When the AAA diameter is more than 5.5 cm for a male or 5cm for a female [6], he/she is recommended to accept surgery.

As an important branch of biomechanics, Biofluid combines of the biology, medicine, physiology, bioengineering, biomedical engineering and fluid mechanics. From a few decades ago, Biofluid mechanics developed and focus on the forces and movement of blood cells and whole blood as well as the interaction between blood cells and the vessels wall [7]. A lot of hemodynamics experiments have shown that the creation of aneurysms and varicose veins strongly influence by the blood flow velocity and pressure situations. Vessel wall structure is also important for this creation. In a preliminary study, flow rate ratio, pressure and velocity gradients, and flow behavior were the basic features researched by Biofluid [8]. With the usage of Finite Element Analysis, it

also focuses on velocity distribution, shear stress on the wall, which are leading causes of atherosclerosis.

Hemodynamic factors play a very important role in the formation and development of arterial disease. A large number of experiments on arterial blood flow have made a significant contribution to revealing the hemodynamic mechanism of arterial disease [9].

Science and technology are developing rapidly and steadily, it makes a numerical simulation of the large-scale physical process have been possible, which would greatly simplify the cumbersome and tedious physical experiment processes and solve the problem of expensive experimental costs. In the meantime, complex flow parameters (such as velocity vector, streamline, and wall shear stress) are almost impossible to solve by experiment but can have a good access to numerical simulation. Under the atmosphere of a rapid development of computer techniques, the improved numerical simulation, use the finite element method to calculate and analyze the model is more and more common in nowadays. Computational Fluid Dynamics (CFD) gives an insight into flow patterns that are difficult, expensive or impossible to study using traditional or experimental techniques. These studies might play an important role in improving diagnostics and therapeutic application.

## **1.2 Purpose**

This paper is based on the knowledge of hemodynamics and related disciplines, uses the advanced three-dimensional reconstruction software and the finite element analysis software to compare the healthy abdominal aorta and abdominal aorta aneurysm (AAA). By the approaches of three-dimensional reconstruction, numerical analysis, and simulation, this project is a plan to study the relationship between a variety of forces in blood vessels (such as velocity vector, vessel wall force, wall shear stress) to predict their influences of AAA formation and development. A lot of medical research have shown that AAA has a high mortality and inevitable disability rate. Hence, the potential research results can help the doctor to understand the incidence of AAA and its rupture mechanism, then help people know more about this disease and prevent it in ahead of time.

In recent years, thousands of experiments and research have shown that the blood flow velocity, the pressure, the wall shearing stress and other principal dynamics parameters have important roles in aneurysm pathophysiology. But with the limitation of the experiments and other unavoidable factors (such as high cost, tedious process, high-risk rate, and time-assuming procedure), those parameters are not easy to measure and analyze in the human body.

ANSYS can numerically simulate the aneurysm blood flow in the computer to observe hemodynamics system, which can be used to explore the possible development or rupture mechanism of an aneurysm. It can help doctors to make a correct assessment to the risk of an aneurysm.

In this paper, in one hand, using the printed 3D model to measure and calculate inlet velocity and outlet pressure to observe the blood flow in a physical experiment. On the other hand, used ANSYS to simulate the procedure. Then compare the results between the experiment part and the numerical simulation part. Simulations and comparisons of the healthy abdominal artery and AAA can give information of how blood flow affects the pathology and rupture mechanism of AAA, which can help doctors to design specific treatments for potential patients.

### **1.3 Introduction and Current Development of Relative Filed**

For hemodynamics research and study, using the open source software to simulate is the most common approach. Based on the fact that the red blood cells and diameter of channels are almost on the same order of magnitude, the macro Newton's law cannot be used due to dimensional scales. Instead of that, hemodynamics chooses Lattice-Boltzmann equations or Monte Carlo equations to deal with blood flow problems [10]. Blood flow is characterized by fluid dynamics, which is analyzing and computing by Euler equation with Infinite Volume Analysis and Infinite Element Analysis. There are a lot of commercial software such as ANSYS FLUENT, CFX, ADINA, ABAQUS have been mature and have excellent performances in preprocessing and post-processing for blood flow.

#### **1.3.1 CFD Computational Fluid Dynamics Modeling Analysis**

Computational fluid dynamics (CFD), as an important branch of Fluid Mechanics, uses the numerical analysis and data structure to solve and analyze fluid flow problems, which are calculated and simulated by computer to describe the interaction of liquids and gasses with defined-boundary surfaces [11]. Computational fluid dynamics, which is based on the Navier-Stokes equations, is to visualize how a fluid (gas or liquid) flows or its affect on past flow by the application of applied mathematics, physics, and computational software [12].

CFD provides a qualitative and quantitative prediction of fluid flows by means of mathematical modeling, numerical methods and software tools, which enables scientist and engineers to perform numerical experiments and computer simulations in a virtual flow laboratory.

### **1.3.2 Finite element method**

Finite element is derived from mechanics and is a discrete numerical method [13]. In 1870, the British scientist Rayleigh solved complex differential equations with the usage of hypothetical “test function”. In 1909, Ritz developed it into a perfect numerical approximation method, which laid a sound foundation for the modern finite element method. In 1967, Sienkiewicz and Cheung published first Finite element analysis book.

The research of the finite element method is mainly used to solve the problem in structural mechanics, and now is also widely used in the numerical solution of fluid mechanics. The basic idea of finite element method is to separate the continuous geometric area into a finite number but non-overlapping finite units then set the basic function and use finite numbers of unknowns to approximate the infinite unknown real system [14].

In the hemodynamics, many problems are difficult to get an accurate solution, even the engineering models are complex. Although the finite element method merely to obtain the similar results, the increasing numbers of units and rationality can improve the accuracy of the results obtained. This high precision and developing accuracy make it an effective means of analysis in nowadays engineering analysis.

Basic steps of the Finite element method for the analysis of blood vessel:

1. Problem Recognition and Domain Definition
2. Discretization of the Structure

The area of the blood vessel flow calculation is divided into finite numbers but not overlapping solution units. And the cells are only connected at the nodes, making it a continuous system of element geometry.

3. Determine the state variables and control methods

Set the speed as constant.

4. Units analysis
5. Overall analysis

The most important feature of Finite Element Analysis is standardization, which makes it possible for large-scale analysis and calculation. With the help of the modern computer and related finite element analysis software, the large-scale analysis of complex engineering problems becomes a reality. The rapid development of computer technology generates a large number of finite element analysis software, which provides complete convenience for all kinds of engineering researches

and developments. Nowadays, there is many professional commercial finite element analysis software are ANSYS, ANAQUUS, ALGOR, COSMOL and etc.

In this paper, ANSYS is used to study the blood flow and pressure distribution in both healthy abdominal arteries and abdominal aneurysms, so as to understand and analyze the formation and rupture mechanism of AAA.

### **1.3.3 Hemodynamics**

Hemodynamics is the dynamics of blood flow. It is an important part of cardiovascular physiology dealing with the forces the heart has to circulate blood through the cardiovascular system [15]. Blood, which makes up approximately 8% of an adult's body weight, is classified as a connective tissue and consists of Plasma (which is a clear extracellular fluid) and Formed elements (which are made up of the blood cells and platelets) [16]. Hemodynamics explains how blood flows in the vessels and corresponding governing physical laws.

Human Blood is a non-Newtonian fluid and has the laminar characteristic. Blood flow velocity is the fastest in the middle of the vessel and slowest at the vessel wall [16, 17].

The viscosity of blood flow will be thinner alongside the shearing stress. In the high flow rate and high shear strain place, the viscosity of the blood increases, which makes the blood flow performs more uniformly.

Kumar developed a simple ideal geometric model to obtain an analytical solution in a long time ago.

However, those models which were using in the hemodynamic experiments were limited to the velocity and pressure. But they were hard to get more complex hemodynamic parameters, such as velocity vector, streamline, contours, shearing stress and etc.

With the rapid development of computer technology and calculation methodology, numerical simulation by computer or even supercomputers has been an indispensable means of research. The high-precision and high-accuracy hemodynamic numerical simulation must rely on anatomically accurate vascular geometry or geometrical models obtain by Computer tomography. The hemodynamics numerical simulation only can help people understand atherosclerosis if based on the virtual blood flow with considerations comprehensively of wall shear stress, particle retention time and oxygen cross-vascular wall transmission.

### **1.3.4 Three-Dimensional Printing (3D Printing)**

Three-Dimensional Printing (3D Printing), which is a rapid prototyping technology, is a layer-by-layer process of making three dimensional solid objects based on a digital model file by using powdered metal, plastic or other adhesive materials [18]. In 1986, the first commercial 3D printer had been developed by an American scientist - Charles Hull. After that, 3D printing technology is becoming more and more familiar with the world.

The 3D printer has same basic operating principles as the ordinary printer, but they have different printing materials. The ordinary printer uses ink and paper while 3D printer works with metal, ceramic, plastic, sand and other materials, which are real raw material [19]. When connects the printer with the computer, the printing material can be overlay regularly through computer control, that makes the blueprint change to solid objects.

The complex 3D model can be more easily manufactured with the 3D printers by transforming in a series of two-dimension fabrication overlays, which make it possible to generate any complex parts without the use of molds and tools and greatly improving the productivity and manufacturing flexibility.

The commonly used materials for 3D printing are nylon-glass fiber, durable nylon materials, gypsum materials, aluminum material, titanium alloy, stainless steel, silver, gold, rubber materials.

3D Printing design Process:

1. Modeling the objects by computer modeling software.
2. Slicing the three-dimensional model into a series of layers.
3. Controlling the printers to print layer by layer.

The standard collaboration format between the design software and the printer are the STL files.

### **1.3.5 Overview of ANSYS**

ANSYS, Inc., which was founded in 1970, is dedicated to engineering simulation software and technology research [20]. ANSYS is wildly used by all over the world by engineers and designers in many industries. FLUENT. Inc., the leader in the field of fluid simulation, was acquired by ANSYS. Inc., in 2006 [21].

ANSYS software is a large-scale general-purpose Finite Element Analysis (FEA) software which developed by ANSYS. Inc. It is also the fastest growing Computer-Aided Engineering (CAE) software in the world. ANSYS can interface with most commuter-aided design software (such as CAD, Creo, NASTRAN, Alogor and etc.) to achieve data sharing and exchange [22].

ANSYS software, which has become the most popular international finite element analysis software, is powerful and easy to operate.

Nowadays, ANSYS has an entire product line includes ANSYS Mechanical series, ANSYS CFD (FLUENT/CFX) series, Electronic Design (ANSYS ANSOFT) series, ANSYS Workbench and EKM [23]. The software provides more than 100 types of simulation cells to simulate the various structures and materials in engineering.

ANSYS mainly includes three stages: the Pre-processing module, the analysis-calculation module, and the post-processing module [24].

#### 1. Pre-processing Module

This module provides a powerful solid modeling and meshing tool that allows the user to easily construct a finite element model. Firstly, build a geometric model. Secondly, establish a finite element model, the select unit and define materials. Then, use the meshing tool for this finite element model.

#### 2. Analysis-Calculation Module

This module includes structural analysis (linear analysis, nonlinear analysis, and highly nonlinear analysis), hydrodynamic analysis, electromagnetic field analysis, sound field analysis, piezoelectric analysis and coupling analysis of multi-physical fields. They can simulate interactions among a variety of physical media with sensitivity analysis and optimization analysis capabilities.

#### 3. Post-processing Module

This module can display in color contours, gradient, vector, particle flow, stereoscopic sections (transparent or translucent), streamline and etc. The results also can be exported or displayed as graphs or curves.

### **1.4 Main Content**

This paper focuses on the flow of blood in the abdominal arteries and uses the finite element method to simulate the blood flow by ANSYS FLUENT.

In this paper, healthy abdominal aorta model and abdominal aortic aneurysm model were established, which were calculated and analyze by ANSYS FLUENT. With post-processed stages of the analysis, the corresponding blood flow and blood pressure distribution were shown.

At the same time, the numerical simulation results were compared with the physical experimental which was based on the respective 3D printing model.

The main purpose is to study the relationship between the force in the blood vessel wall and the effects of various forces such as wall shear stress on the formation and growth of abdominal aneurysms.

There are several tasks finished in this project:

#### Part One - Numerical Simulation

- I. Preprocessing
  - a. Define the geometry and physical bounds.
  - b. Data can be suitably processed (cleaned-up).
  - c. Extract the fluid volume (or fluid domain).
  - d. Mesh
- II. Analysis
- III. Use ANSYS to simulate the velocity and pressure in two models: healthy one and AAA one.
- IV. Result
  - a. Velocity: Vector field, Streamline
  - b. Pressure: Vector Filed, Streamline, Contour and Wall artery pressure distribution
  - c. Shear: Contour and Wall artery shear distribution

#### Part Two – 3D model and Experiment

- I. 3D model
  - a. Build the CAD model files of the healthy abdominal artery and AAA.
  - b. Use the 3D printer to print two models
  - c. Design the experiment boundary condition
- II. Conducting Experiment

#### Part three - Compare and Result

Compare simulation and experiment result, obtain the conclusion about the factors which affect AAA formation and rupture mechanism.



## 2. Two Mathematical Techniques and Numerical Analysis

### 2.1 Non-Uniform Rational B-spline Surface (NURBS)

In this paper, use Geomagic Studio 12 to smooth the surface of the scanned blood vessel model, in which uses NURBS surface smoothing [25].

Non-Uniform Rational B-spline (NURBS) is a rational B-spline function allowing a non-uniform knot vector [26]. NURBS generalize the B-spline curves which can combine the parametric curves and the analytical curves in a single form.

The definition of NURBS is shown as following equation:

$$C(u) = \frac{1}{\sum_{i=0}^n N_{i,p}(u)w_i} \sum_{i=0}^n N_{i,p}(u)w_i P_i \quad (\text{Eq. 2-1})$$

$$P_i = \begin{bmatrix} x_i \\ y_i \\ z_i \\ 1 \end{bmatrix} \quad (\text{Eq. 2-2})$$

This equation is the NURBS curve of degree  $p$ , which is defined by control points  $P_0, P_1, \dots, P_n$ , knot vector  $U = \{u_0, u_1, \dots, u_n\}$ , and weights  $w_0, w_1, \dots, w_n$ .

The most widely used techniques for modeling of general surfaces (including free-form surfaces) are extensions into the second parametric dimension of the polynomial curve techniques. The mathematical basis of the techniques is basically an extension of that of the curve forms. Similar to the fact that curve segment is the fundamental building block for curve entities, the patch is the fundamental building block for surfaces. Therefore, piecewise continuous surface patches can be used to represent surfaces.

A plane can be described by three points (e.g.  $P_0, P_1$ , and  $P_2$ ). The NURBS formulation requires the definition of a fourth point:

$$P(u, v) = \sum_{i=0}^1 \sum_{j=0}^1 P_{ij} R_{i,k}(u) R_{j,l}(v) \quad (\text{Eq. 2-3})$$

$$0 \leq u \leq 1, 0 \leq v \leq 1 \quad (\text{Eq. 2-4})$$

The fourth point,  $P_{11}$  is defined as a linear combination of three points  $P_0, P_1$ , and  $P_2$ :

$$P_{11} = (P_1 - P_0) + P_2 \quad (\text{Eq. 2-5})$$

$$P_{11} = (P_2 - P_0) + P_1 \quad (\text{Eq. 2-6})$$

The general form of NURBS equation can be represented as follows:

$$P(u, v) = \frac{1}{\sum_{i=0}^1 \sum_{j=0}^1 w_{ij} w_{ij} N_{i,2}(u) N_{j,2}(v)} [w_{00} w_{00} P_{00} N_{0,2}(u) N_{0,2}(v) + w_{01} w_{01} P_{01} N_{0,2}(u) N_{1,2}(v) + w_{10} w_{10} P_{10} N_{1,2}(u) N_{0,2}(v) + w_{11} w_{11} P_{11} N_{1,2}(u) N_{1,2}(v)] \quad (\text{Eq. 2-7})$$

## 2.2 Governing Equation

Fluid (gas and liquid) flows are governed by partial differential equations which represent conservation laws for the mass, momentum, and energy. The human blood is a viscous incompressible fluid, which is generally described by the continuous equation of velocity divergence of zero (also known as the incompressible equation) and the famous Navier-Stokes equation in fluid mechanics. Navier-Stokes equations (N-S equations) are the governing equations of fluid motions, which are based on mass conservation, Newton's 2nd law, and energy conservation [27]. N-S equations describe how the velocity, pressure, temperature, and density of a moving fluid are related. They are composed of partial differential derivatives in time and space.

### 2.2.1 Reynolds number

The Reynolds number,  $Re$ , is a dimension number interpreted as the ratio of inertial forces to viscous forces in the fluid [28].

The viscosity of a fluid is a measure of that fluid's resistant to flow when acted by an external force.

$$Re = \frac{vD\rho}{\mu} = \frac{vD}{\nu} \quad (\text{Eq. 2-8})$$

When the Reynolds number is less than approximately 2100, the flow is said to be Laminar flow; when it is greater than 4000, the flow is said to be Turbulent flow; when the Reynolds number is between 2100 and 4000, the flow is said to be in critical zone or transition region. Hence, we called 2100 and 4000 as critical Reynolds number [29].

Non-Newtonian fluids have viscosities that change with shear rate,  $dv/dt$ .

With laminar flow in a circular pipe, viscosity makes some fluid particles adhere to the wall. If assuming human blood as laminar flow and blood vessel as circular pipe, which followed the flow distribution phenomenon, the closer to the blood vessel, the greater the tendency will be for the fluid to adhere.

### 2.2.2 Navier-Stoke Equations

Human blood is Non-Newtonian fluid, while the blood flow is a slow velocity, incompressible and viscous laminar motion.

Navier-Stokes equations describe the dynamic equilibrium of the force on any given region of the fluid substances (liquids and gasses), and its viscous fluid motion differential equation can be used to describe the flow of viscous incompressible fluid.

This paper used N-S equation to control and simulate the blood flow in the arteries [30].

Naiver-Stokes equation's generally expressed as:

$$\rho \left( \frac{\partial \mathbf{u}}{\partial t} + \mathbf{u} \cdot \nabla \mathbf{u} \right) + \nabla \cdot \mathbf{p} - \nabla \cdot \boldsymbol{\tau} - \mathbf{F} = 0 \quad (\text{Eq. 2-9})$$

In this equation,  $\mathbf{u}$  is flow velocity,  $\rho$  is the fluid density,  $p$  is the pressure,  $\boldsymbol{\tau}$  is the deviatoric component of the total stress tensor,  $\mathbf{F}$  represents body forces in the fluid,  $\nabla$  is Del operator.

The general form of how N-S equation describe the human blood flow can be expressed as:

Equation:

$$\rho \frac{\partial \mathbf{u}}{\partial t} + \rho(\boldsymbol{\mu} * \nabla) \mathbf{u} - \boldsymbol{\nu} \cdot \Delta + \nabla \cdot \mathbf{p} = \mathbf{F} \quad (\text{Eq. 2-10})$$

In this general form of equation,  $\rho$  is the density of the fluid ( $\text{g/cm}^3$ ),  $\boldsymbol{\nu}$  is the viscosity of the fluid ( $\text{g/(cm}^2 * \text{sec})$ ),  $p=p(x, y, t)$  is the pressure at the point  $(x, y)$  at time  $t(\text{g/(cm}^2 * \text{sec)})$ ,  $\mathbf{F}$  is any external forces acting on the fluid.

Blood is a viscous fluid, the continuity function can be expressed as:

$$\frac{\partial \rho}{\partial t} + \nabla \cdot (\rho \mathbf{u}) = 0 \quad (\text{Eq. 2-11})$$

In this equation,  $\mathbf{u}$  is the flow velocity of one specific point,  $\rho$  is the density.

Based on the fact that blood flow is viscous and incompressible, the equation (2-3) can be simplified as below [28]:

$$\nabla * \mathbf{u} = 0 \quad (\text{Eq. 2-12})$$

In order to seek the relationship between fluid shear stress and deformation rate, Stokes made three basic assumptions with the analogy of Hooke law in mechanical materials.

The third assumption in Stokes law is: in the static fluid field, the shear stress is zero while each normal stress equals static pressure [31]

$$\sigma_{xx} = \sigma_{yy} = \sigma_{zz} = -p \quad (\text{Eq. 2-13})$$

Blood flow velocity changes alongside with motion direction, which generates the additional viscous normal stress.

$$\Delta \sigma_{xx} = 2\mu \frac{\partial u}{\partial x} - \frac{2}{3}\mu \nabla \cdot \mathbf{V} \quad (\text{Eq. 2-14})$$

$$\Delta \sigma_{yy} = 2\mu \frac{\partial v}{\partial y} - \frac{2}{3}\mu \nabla \cdot \mathbf{V} \quad (\text{Eq. 2-15})$$

$$\Delta \sigma_{zz} = 2\mu \frac{\partial w}{\partial z} - \frac{2}{3}\mu \nabla \cdot \mathbf{V} \quad (\text{Eq. 2-16})$$

Where,

$$\nabla \cdot \mathbf{V} = \frac{\partial v_x}{\partial x} + \frac{\partial v_y}{\partial y} + \frac{\partial v_z}{\partial z} \quad (\text{Eq. 2-17})$$

$$\tau_{xy} = \tau_{yx} = \mu \left( \frac{\partial v}{\partial x} + \frac{\partial u}{\partial y} \right) \quad (\text{Eq. 2-18})$$

$$\tau_{yz} = \tau_{zy} = \mu \left( \frac{\partial w}{\partial y} + \frac{\partial v}{\partial z} \right) \quad (\text{Eq. 2-19})$$

$$\tau_{zx} = \tau_{xz} = \mu \left( \frac{\partial u}{\partial z} + \frac{\partial w}{\partial x} \right) \quad (\text{Eq. 2-20})$$

Hence, the viscous flow motion equation expressed by stress is

$$\rho \frac{\partial v}{\partial t} = \rho g - \nabla p + \mu \nabla^2 V \quad (\text{Eq. 2-21})$$

Because of the existence of the viscous of normal stress, the pressure of flow fluid is not numerically equal to the normal stress.

In those equations, the thermal influences are not considered.

Hagen-Poiseuille equation describes the flow rate of laminar flow in a circular pipe.

### 2.3 Tetrahedron and Hexahedron

The volume occupied by the fluid is divided into the mesh, which may be uniform and non-uniform, structured and unstructured. The mesh consists of a combination of hexahedral, tetrahedral. Prismatic, pyramidal or polyhedral elements [32].

In 1992, A.O Cifuentes and A. Kalbag concluded that Tetrahedral and hexahedral meshing were equivalent in terms of both accuracy and even in CPU time. However, with time flies and computer sciences develops, there are a lot of experiments have shown that Tetrahedral (TET) and Hexahedral (HEX) have their own advantages. Both Tetrahedral and Hexahedral can provide excellent strain solution by a rational degree of freedom and reliable unit meshing. The hexahedral mesh is more beautiful than Tetrahedral. Hexahedral has a higher precision theoretically with fewer nodes in the same magnitude geometry. For Tetrahedral, it can solve a more complex solid geometry, which guarantees an appropriate mesh quality and makes sure the simulation reliability. It allows the user to deal with mesh unit conveniently in a short time.

In this paper, the blood vessel model used have a complex surface condition, and the purpose is to study the influence of shear stress applied to vessel surface. Hence, surface condition details cannot be ignored and should be considered while doing the simulation calculation. Tetrahedral provides a better approach in this situation. Though Hexahedral can provide a higher calculation precision, it is hard to generate the hexahedral mesh with the irregular blood vessel model.

### **3. Three Image Reconstruction and Establishment of Vascular Flow Model**

#### **3.1 3D Reconstruction of the blood flow area --- Boolean Rules**

In the Boolean operation, a series of data can be dealt with into logic calculation, such as intersection, union, subtraction and etc. ANSYS provides users the Boolean operation module for the solid model, in order to change or create a new model shape in a short time. Boolean operation can be applied to the geometric model. In ANSYS, Boolean operation includes INTERSECTION, OVERLAP, DIVIDE, GLUE, ADD, SUBTRACT and etc [33]. They are not only appropriate for simple geometric unit but also for complex geometric solid model from CAD system.

In this paper, SUBTRACT operation is used to generate the blood vessel wall (3D model for physical experiment):

- A. Define blood flow area (I) and create a corresponding cylinder model (II) which can involve the whole blood flow area.
- B. Read (I) and (II) and establish the information of these two enclosed model.
- C. Confirm that (II) includes (I) and test whether or not contains the intersection between them.
- D. With the SUBTRACT operation and get the model as (II)-(I), which is used for physical experiment.

The original model is the blood flow area without carotid wall, which is the reason using Boolean operation to get an empty part (Blood flow area) in the cylinder model.

#### **3.2 Reverse Engineering --- Geomagic Studio 12**

Reverse engineering is the general term of the digital technique, geometric model reconstruction technique and product manufacturing techniques, which are about how to obtain mathematical models from physical samples and convert them into CAD models [34]. Reverse Engineering is based on the innovation ideas of product introduction, digestion and absorption, the working framework as “solid, design intent, 3D reconstruction, Redesign”, then transform the existing product or solid model into engineering design model and conceptual model.

Geomagic Studio can be used to transform the three dimensional data and polygonal meshes into precisely curved 3D digital model, which is applied for product design and analysis in reverse engineering. As the fastest way to convert the SD scanned data into parametric CAD model and 3D CAD model, Geomagic Studio has powerful reverse modeling function with high efficiency, which also provides a multi-dimensional output format. Geomagic Studio follow the three-stage

workflow as “Point – Polygon Phase – NURBS Surface Phase”, which can easily create the perfect polygon model and tetrahedral mesh from the point cloud and transform it into NURBS surface.

Geomagic studio Reverse Engineering technology process:

1. Import the STL files, read the geometric model
2. Preprocessing:
  - a. Follow the recommending step to use the Mesh Doctor to analyze and repair the polygon mesh.
  - b. Data stitching, simplification, triangulation, denoising.
  - c. Modify editing and cleaning polygon models
3. Blocking
  - a. Choose the appropriate Curvature Sensitivity, Separator Sensitivity to compute and detect contours.
  - b. Reconstruct and repair patches.
  - c. Contracture grids.
4. NURBS surface fitting
5. Export the model into expected format

In this project, export the IGS files which can be read by ANSYS FLUENT.



*Figure3. 1 NURBS surface of healthy abdominal artery*

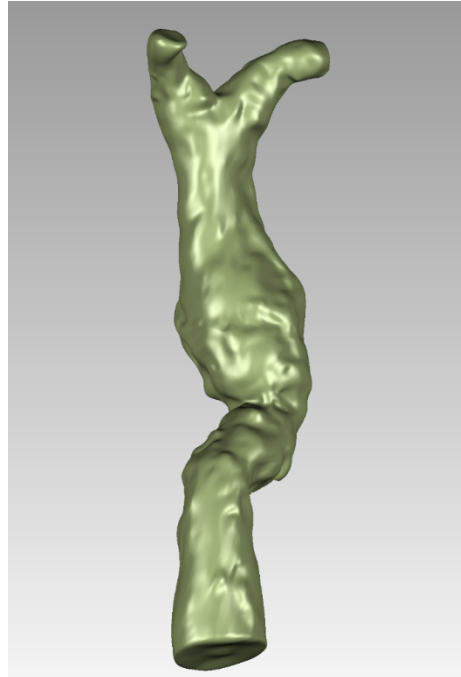


*Figure3. 2 NURBS surface of AAA model*

### 3.3 Mesh

ANSYS, as the most famous commercial and professional finite element analysis software, it can automatically generate tetrahedral mesh in a short time. ANSYS meshing method can be divided simply into two kinds: Free meshing and Mapping meshing.

Free meshing can easily establish the solid model without tedious limitations. When doing the free meshing, the system can generate mesh automatically with combination of different unit type and density. The rationality of mesh, which is the grid quality, affects the calculation accuracy.

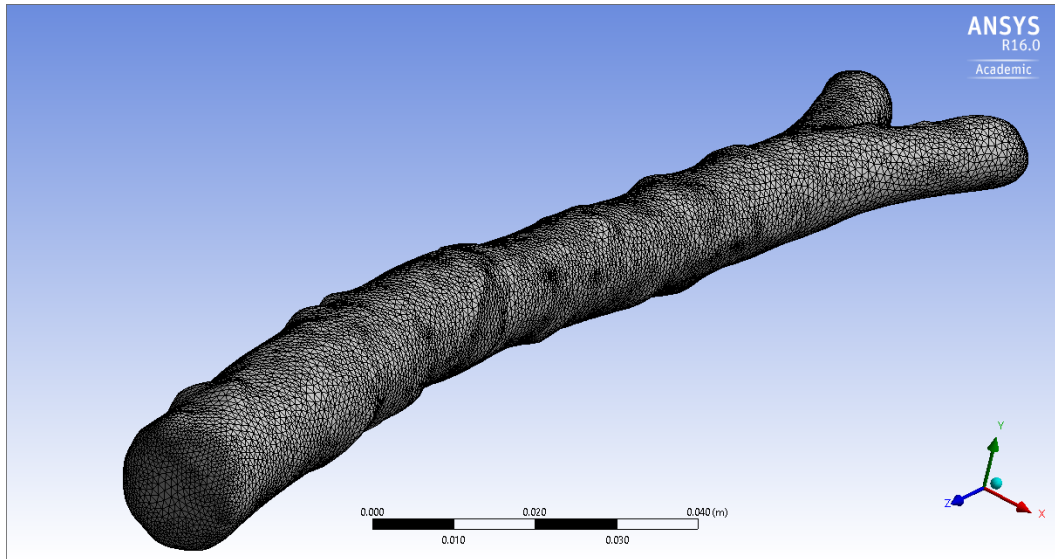


Figure3. 3Mesh of the healthy Abdominal Artery model

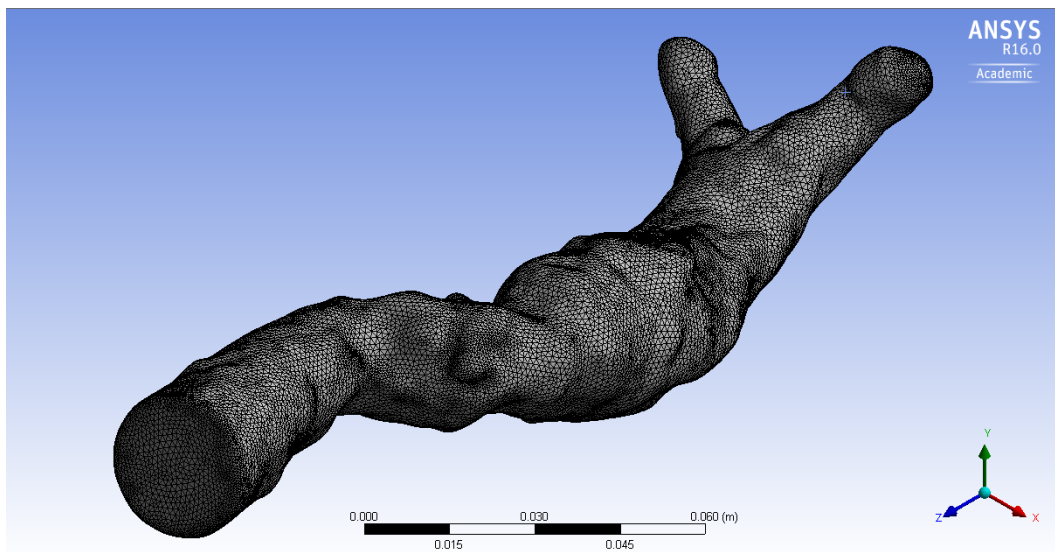


Figure3. 4 Mesh of the AAA model

### 3.4 Numerical realization

In this section, we used ANSYS FLUENT to simulate the blood flow at the abdominal artery.

It is known as that ANSYS finite element method idealizes a continuous system with finite numbers of non-overlapping units instead of a continuous system with an infinite number of degree of freedom. ANSYS also has a wide range of applications, which can handle complex models and complex boundaries in a various engineering field, which is very convenient for numerical simulation of blood vessel flow model. The visualization of ANSYS numerical processing results makes all related study more room for development.

In this paper, ANSYS FLUENT was used to do the numerical simulation in the blood flow area. The simulating fluid parameters are as followed: Blood density is  $1060\text{kg}/\text{m}^3$ , Infinite Viscosity is  $0.0035\text{kg}/\text{m} \cdot \text{s}$ , and Zero Shear Viscosity is  $0.056\text{ kg}/\text{m} \cdot \text{s}$ . For the boundaries condition, set the inlet with constant velocity as  $0.5\text{m}/\text{s}$ , two outlet have the same constant gauge pressure as 13332 Pascal.



## 4. Experimental Investigation of Blood Vessel Flow in Abdominal Artery

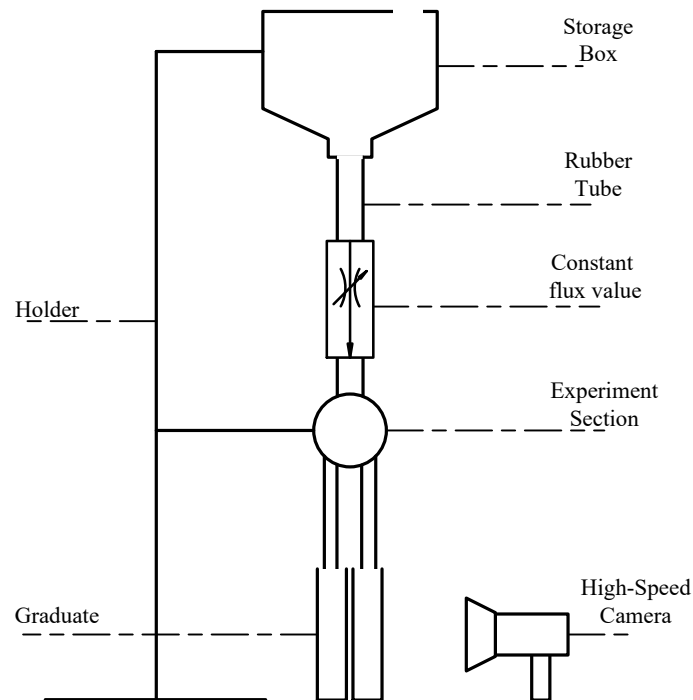
### 4.1 Physical Experiment Parameters Setup

From 1980, there have a lot of research and accomplishment about the blood vessel inlet flow problem. In this paper, in order to focus on the blood velocity and flux for the inlet and two outlets of the healthy abdominal model, there are several assumptions should be consider in this paper: Dynamic similary, Geometric similarity, Physiological similarity, Similar Boundary conditions.

### 4.2 Experiment Device Design

#### 4.2.1 Experiment Device Design Method

In this section, used the 3D printing technique produce a healthy blood vessel model. Design a physical experiment to measure the flux of two outlets. The following figure are the experiment conducted for this paper.



The Experiment Device contains the following Components:

- (i). Holder: Support the whole device.
- (ii). Storage Box: Storage the analog liquid of blood.

- (iii). Rubber Tube: Connect the Storage Box, Constant Flux Value and Experiment section, also conduct the flow from two outlets of 3D printer's model to two separate graduate.
- (iv). Constant Flux Value: Control the analog liquid.
- (v). Experiment Section: Use the 3D printing model of healthy abdominal vessel as the analog blood vessel, simulate how blood flow in the vessel.
- (vi). Graduate: Measure the flow flux of two outlets, respectively.
- (vii). High-Speed Camera: Record how the flow into graduates changed by time.

#### 4.2.2 Photos of Experiment Device

In this experiment, print out the 3D model of Healthy abdominal artery, use the water as the analogy blood, which has the similar density as human blood.

Set the inlet has a constant velocity as 0.1m/s and measure the rate of the flow from the right outlet to the left one during a same period.

The data will compare with the numerical simulation one.



Figure5. 1 Device 1

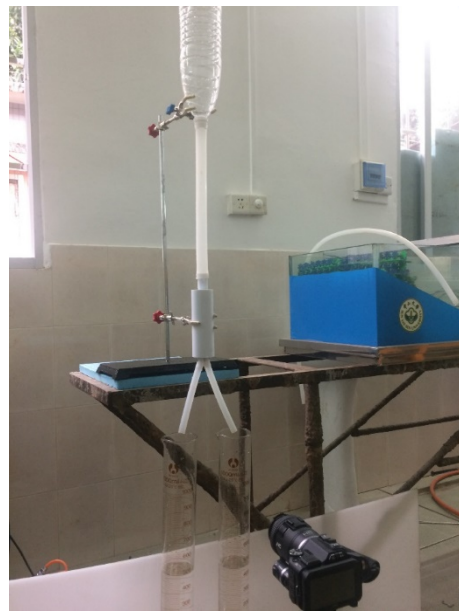


Figure5. 2 Device

### 4.3 Experiment Results

The following table is the data measured by the designed device above.

Left Flow ml	Right Flow ml	Modified Left	Modified Right	Right/Left
770	665	758.5	652.4	0.860118655

## **5. Numerical Investigation of Blood Vessel Flow in Abdominal Artery**

In this part, the velocity, pressure and shear stress are three important factors need to be calculated and analyzed. There are several kinds of result figures shown in this section: Velocity Vector, Velocity Streamline, Pressure Vector, Pressure Distribution (Fluid zone), Artery Wall Pressure Distribution, Pressure Contour, Artery Wall Shear Stress Distribution, and Artery Wall Shear Contour.

In order to compare the different blood flow situation between healthy abdominal artery (left one) and aneurysm (right one), each comparison contains two selected directions. One is the Default orientation and the other one is Specific Orientation, which is chosen as the output outward to specify exactly what happens there.

From those figures, people can see the change of pressure and shear stress in the artery wall easily and directly. The result and the conclusion can help people know the formation and rupture mechanism of the abdominal aneurysm.

## 5.1 Velocity Simulation Results

### 5.1.1 Comparison of Velocity Vector Field

Velocity Vector Field shows the velocity magnitude and direction of each point in the blood fluid zone.

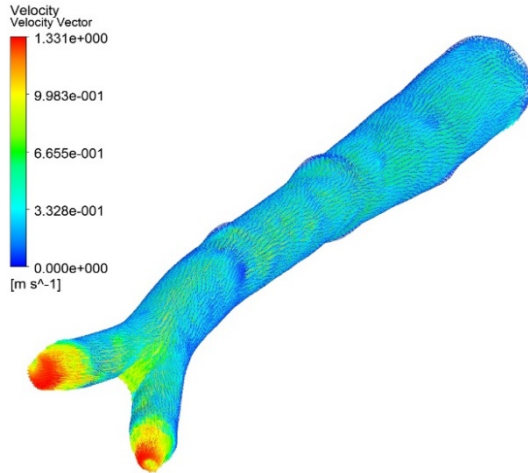


Figure4. 1 Velocity Vector Distribution of Healthy Abdominal Artery (Specific Orientation)

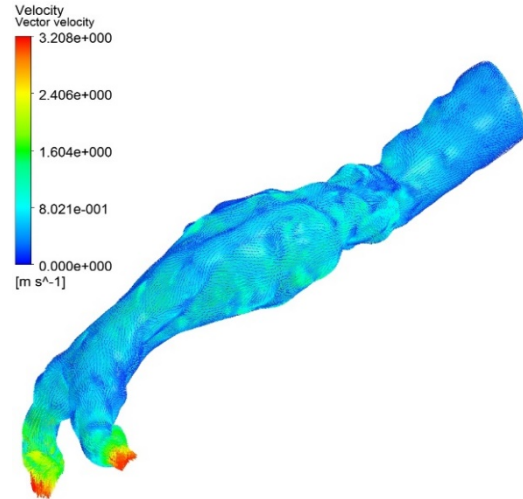


Figure4. 2 Velocity Vector Distribution of Abdominal Aneurysm (Specific Orientation)

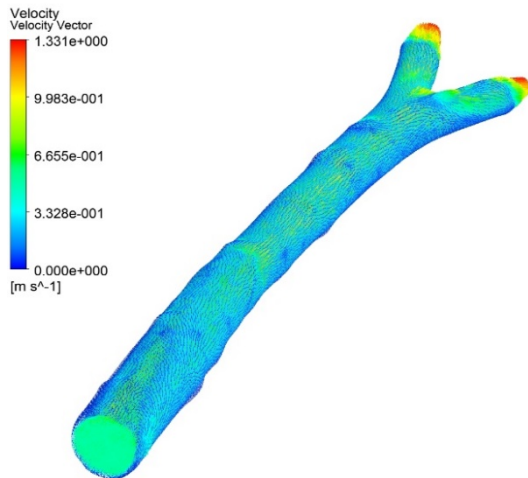


Figure4. 3 Velocity Vector Distribution of Healthy Abdominal Artery (Default Orientation)

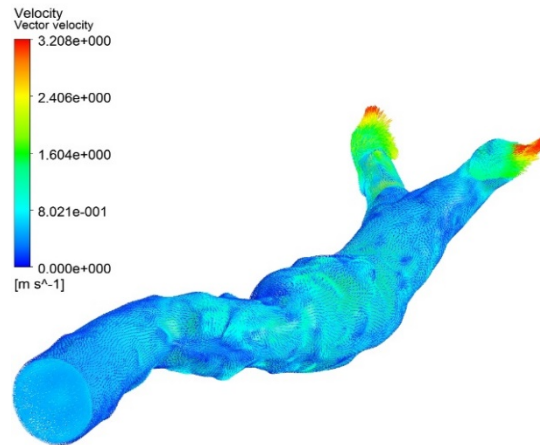


Figure4. 4 Velocity Vector Distribution of Abdominal Aneurysm (Default Orientation)

### 5.1.2 Comparison of Velocity Streamline

Combined of the Velocity vector field and Velocity Streamline, it can provide a more instructive way for people to have a clear sight of how velocity change from the velocity input to the pressure output.

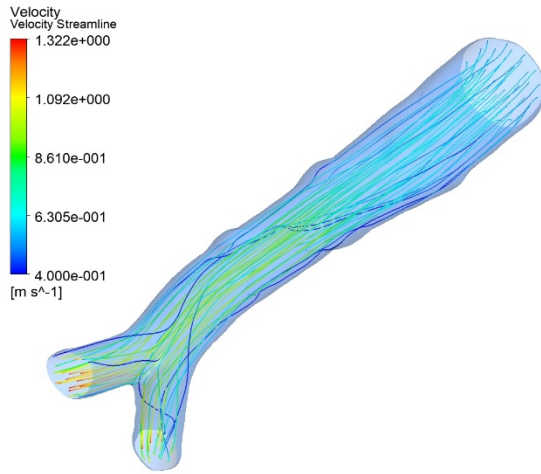


Figure4. 5 Velocity Streamline of Healthy Abdominal Artery (Specific Orientation)

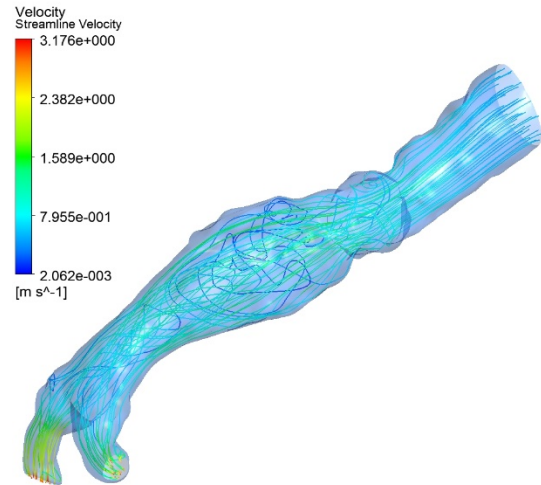


Figure4. 6 Velocity Streamline of Abdominal Artery Aneurysm (Specific Orientation)

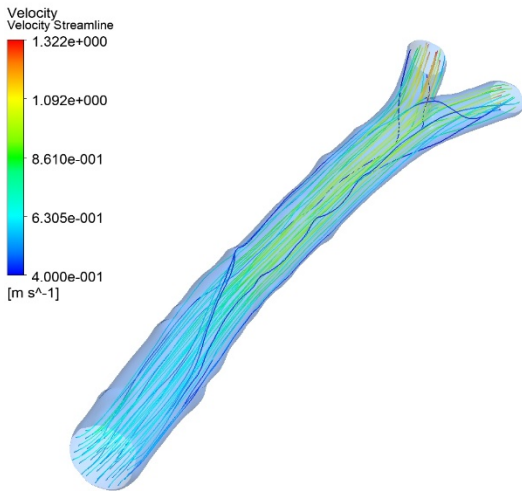


Figure4. 7 Velocity Streamline of Healthy Abdominal Artery (Default Orientation)

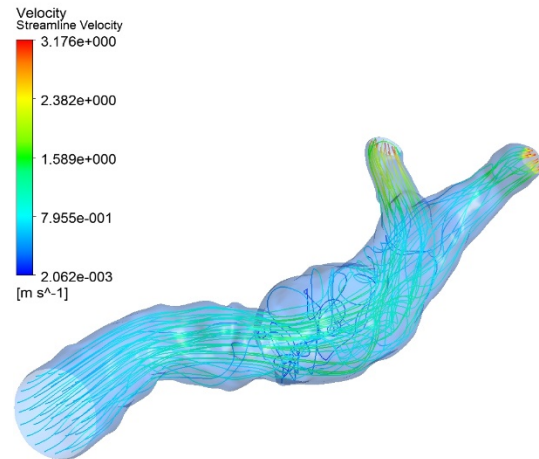


Figure4. 8 Velocity Streamline of Abdominal Artery Aneurysm (Default Orientation)

## 5.2 Pressure Simulation Results

### 5.2.1 Comparison of Pressure Vector Field

Pressure Vector Field shows the pressure magnitude and direction of each point in the blood fluid zone.

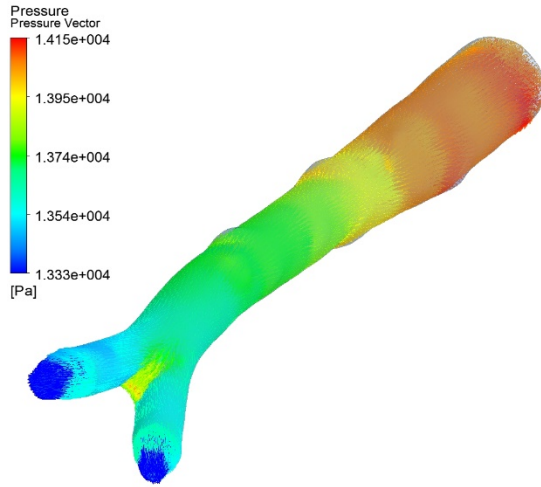


Figure4. 9 Pressure Vector Distribution of Healthy Abdominal Artery (Specific Orientation)

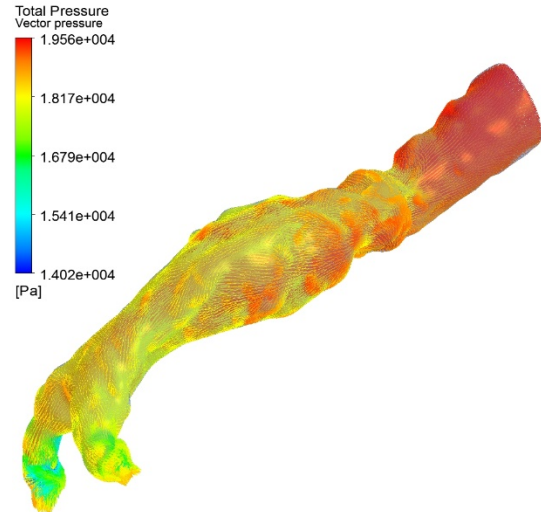


Figure4. 10 Pressure Vector Distribution of Abdominal Artery Aneurysm (Specific Orientation)

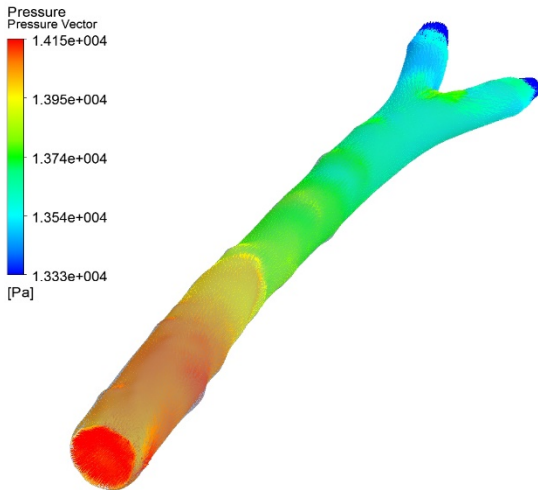


Figure4. 11 Pressure Vector Distribution of Healthy Abdominal Artery (Default Orientation)

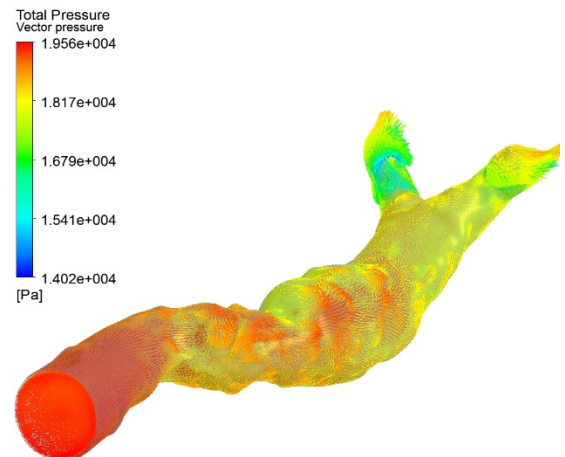


Figure4. 12 Pressure Vector Distribution of Abdominal Artery Aneurysm (Default Orientation)

## 5.2.2 Comparison of how Pressure changes inside the fluid zone

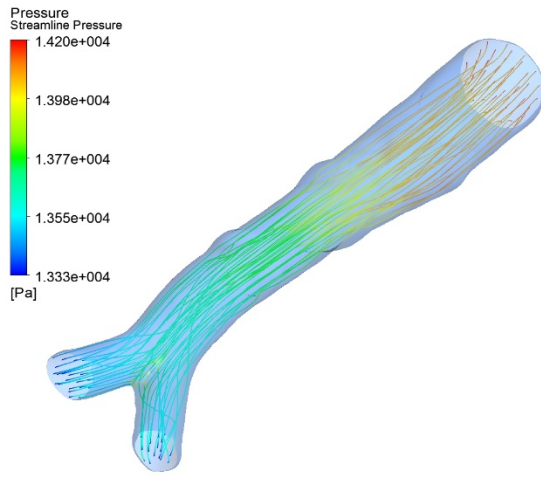


Figure4. 13 Pressure Distribution of Healthy Abdominal Artery (Specific Orientation)

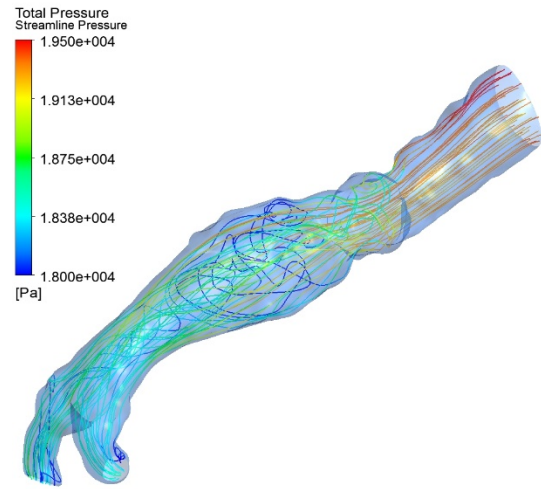


Figure4. 14 Pressure Distribution of Abdominal Artery Aneurysm (Specific Orientation)

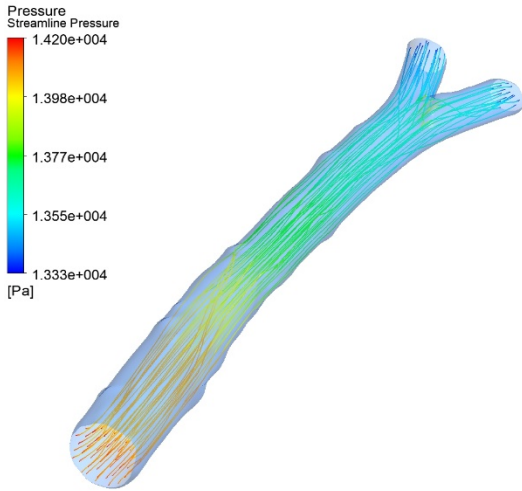


Figure4. 15 Pressure Distribution of Healthy Abdominal Artery (Default Orientation)

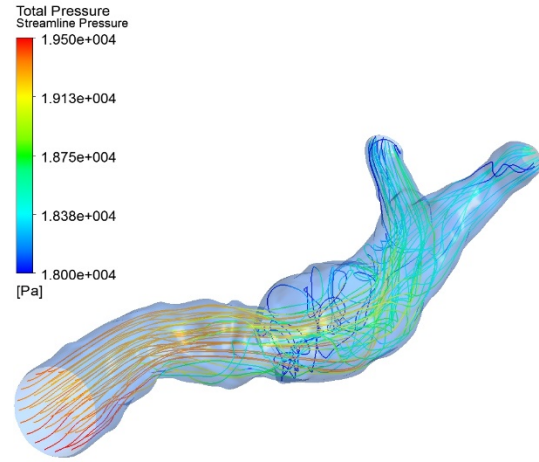


Figure4. 16 Pressure Distribution of Abdominal Artery Aneurysm (Default Orientation)



### 5.2.3 Comparison of Pressure Contour

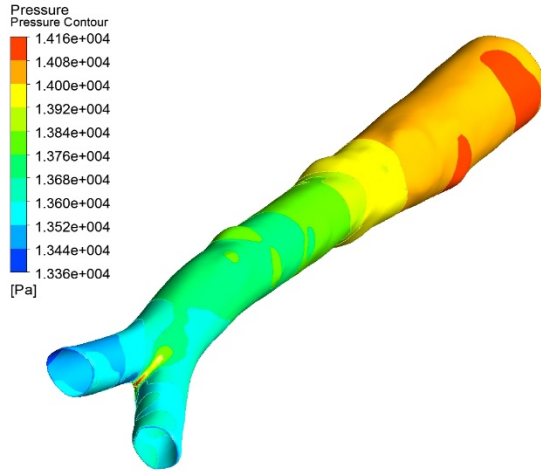


Figure4. 17 Artery Wall Pressure Contour of Healthy Abdominal Artery (Specific Orientation)

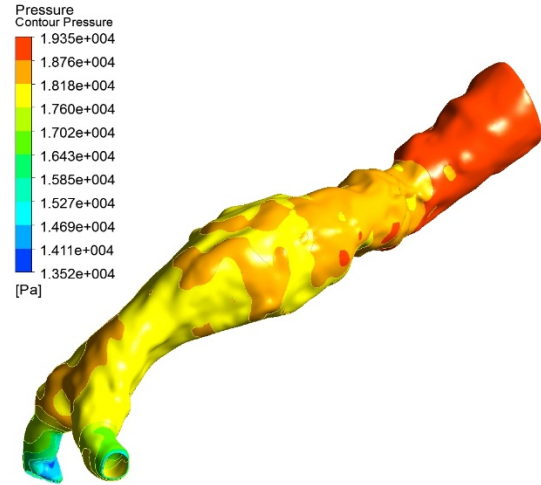


Figure4. 18 Artery Wall Pressure Contour of Abdominal Aneurysm (Specific Orientation)

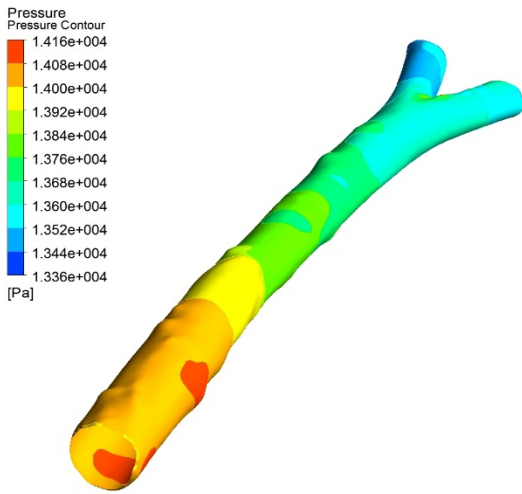


Figure4. 19 Artery Wall Pressure Contour of Healthy Abdominal Artery (Default Orientation)

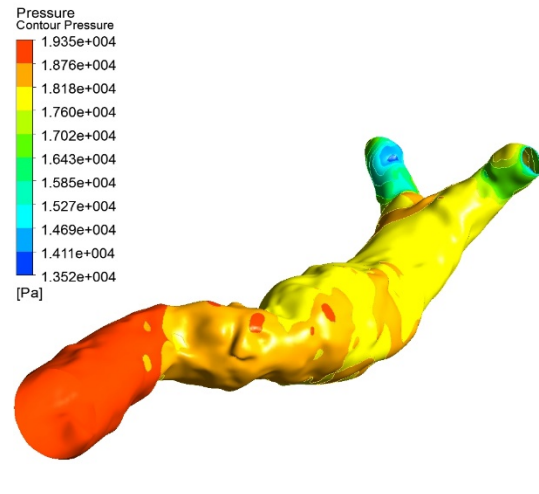


Figure4. 20 Artery Wall Pressure Contour of Abdominal Aneurysm (Default Orientation)



## 5.2.4 Compassion of total pressure at the artery wall

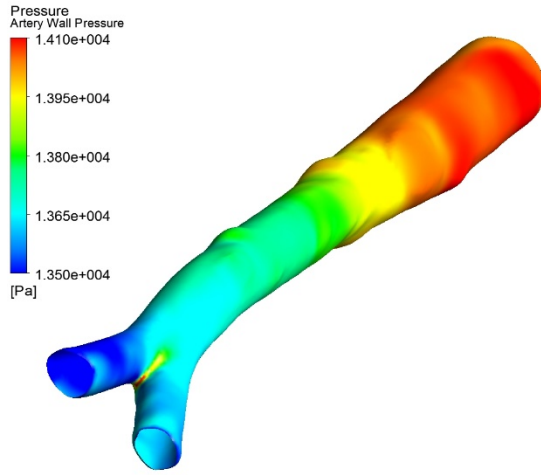


Figure4. 21 Artery Wall Pressure Distribution of Healthy Abdominal Artery (Specific Orientation)

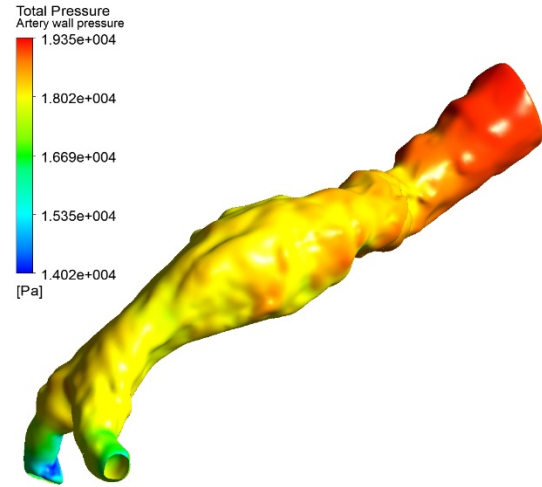


Figure4. 22 Artery Wall Pressure Distribution of Abdominal Aneurysm (Specific Orientation)

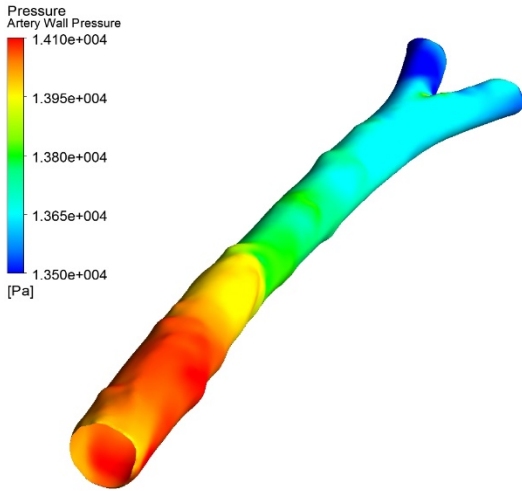


Figure4. 23 Artery Wall Pressure Distribution of Healthy Abdominal Artery (Default Orientation)

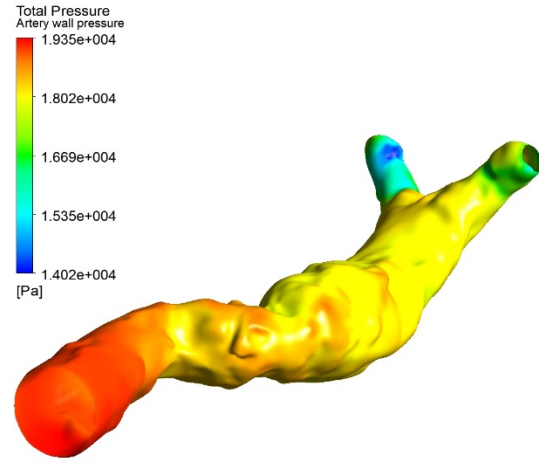


Figure4. 24 Artery Wall Pressure Distribution of Abdominal Aneurysm (Default Orientation)

## 5.3 Wall Shear Stress Simulation Results

### 5.3.1 Comparison of Shear Stress at the Artery wall

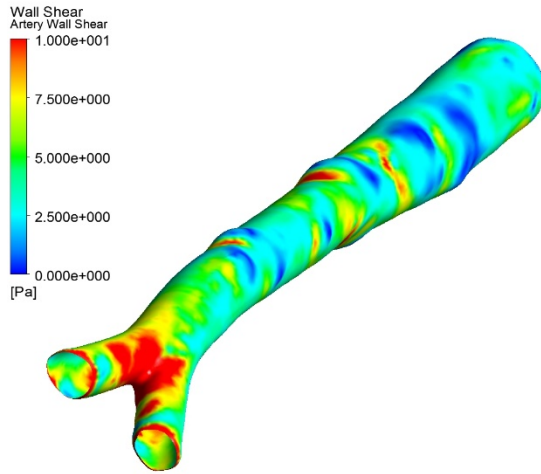


Figure4. 25 Artery Wall Shear Distribution of Healthy Abdominal Artery (Specific Orientation)

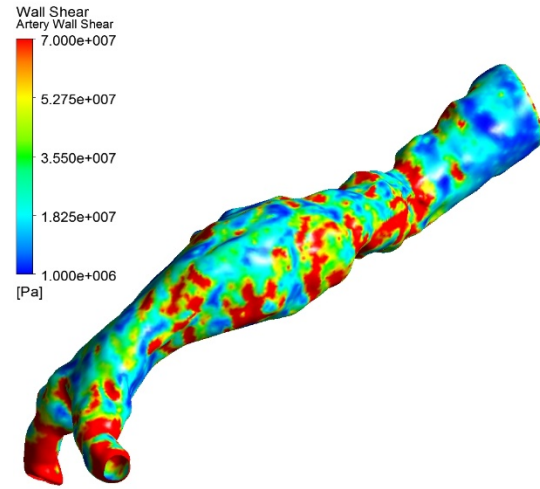


Figure4. 26 Artery Wall Shear Distribution of Abdominal Artery Aneurysm (Specific Orientation)

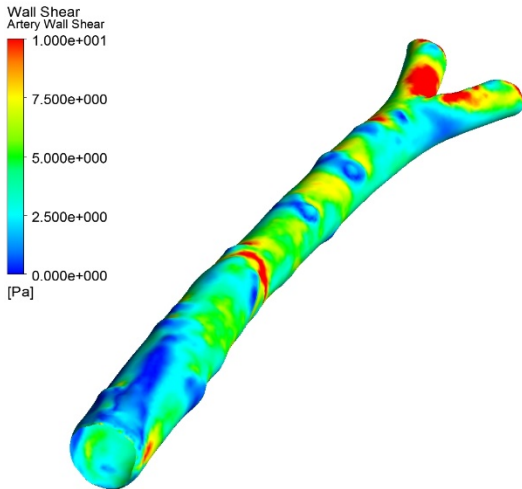


Figure4. 27 Artery Wall Shear Distribution of Healthy Abdominal Artery (Default Orientation)

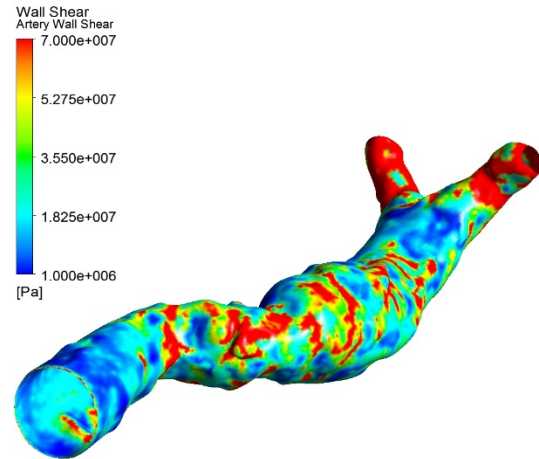


Figure4. 28 Artery Wall Shear Distribution of Abdominal Artery Aneurysm (Default Orientation)

### 5.3.2 Comparison of Wall Shear stress contour.

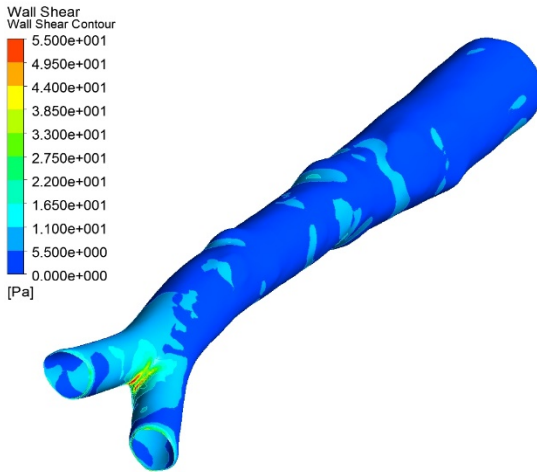


Figure4. 29 Artery Wall Shear Contour of Healthy Abdominal Artery (Specific Orientation)

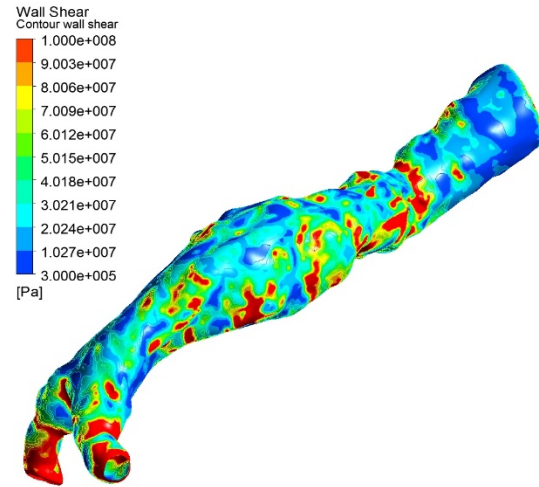


Figure4. 30 Artery Wall Shear Contour of Abdominal Artery Aneurysm (Specific Orientation)

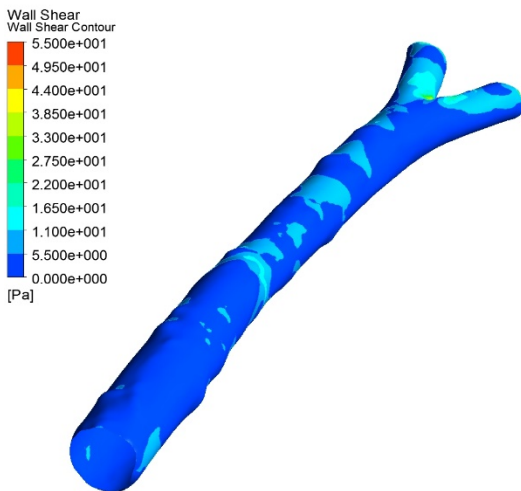


Figure4. 31 Artery Wall Shear Contour of Healthy Abdominal Artery (Default Orientation)

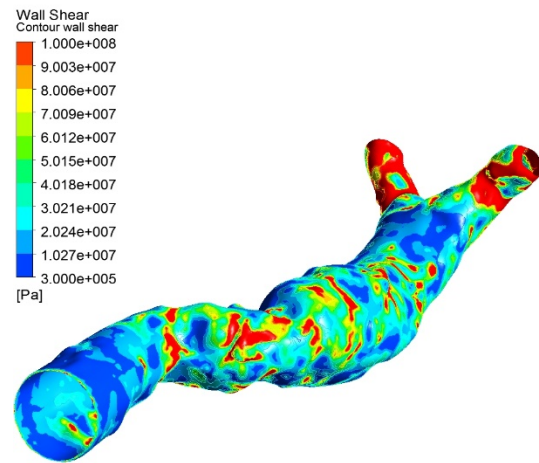


Figure4. 32 Artery Wall Shear Contour of Abdominal Artery Aneurysm (Default Orientation)

## 6. Validation between Physical Experiment and Numerical Simulation with 0.1m/s inlet velocity

Physical experiment results:

Left Flow ml	Right Flow ml	Modified Left	Modified Right	Right/Left
770	665	758.5	652.4	0.860118655

*Table 1. Physical Experiment Result*

ANSYS results:

Left Mass Flow Rate (Kg/s)	Right Mass Flow Rate (Kg/s)	Left flow (ml)	Right Flow (ml)	Right/Left
0.0128299	0.01026296	12103.670	9682.04	0.7999259

*Table 2. Simulation Result*

Relative error:

$$\frac{0.86 - 0.80}{0.80} = 7.5\%$$

The Error here can be accept because it is smaller than 15%.

There are several reasons precipitate this error. Firstly, through the 3D reconstruction, the model surface was smoothed before the blood flow simulation. Secondly, the physical experiment was hard to control the inlet flow rate as a constant. Thirdly, the analogy liquid is water and not a real human blood.

However, the error is within the allowable range, and the similarity between the experiment and the numerical simulation proves that ANSYS has a certain reference for the numerical simulation of the blood vessel flow. Therefore, it can be used to simulate the health model and AAA model with their differences in pressure, Velocity and Shear stress, so as to study the significance of these factors for the pathogenesis of AAA. Those result can provide a reliable reference to the relevant medical field.

## 7. Conclusion and Prospect

N-S equations are the governing formula in this paper, and they are solved based on finite element method by using ANSYS software. Before simulation, the geometry should be obtained via computational tomography (CT) or Magnetic Resonance Imaging (MRI) scanning, and subsequently the vessel structures are smoothed and meshed in Geomagic Studio and Gambit, respectively. The smooth processing is a virtual step for the realization of mesh in this paper as lots of rough boundaries exist in the original images. Nonetheless, more errors are brought into the simulation results because of the uncontrolled changes of geometry. To evaluate the accuracy of hemodynamic results, physical experiments based on 3D print technology are conducted herein. The sizes of models, fluid properties and boundary conditions are all kept same for simulation and experiment.

As the limit of time and the number of original images, we just do the calculation for one model, including healthy one and AAA one, which is not enough to drive precise conclusions. In the near future, more comparisons will be analyzed to get statistic conclusions. To guarantee the calculation speed, unstructured mesh is always used in the current software, which leads to high demanding for geometry shape and smooth. Besides, the used numerical approach is laborious, complex, and error-prone utilizing an ad-hoc coalition of software packages. As we learn from the references, GPU-accelerated lattice Boltzmann method (LBM) is a recommending alternative method for the bleed flow simulation. This method has a lower limit for the model shape and perfect GPU parallel structure of mathematical method can dramatically shorten the calculation time by parallelization. Last but not least, the experiment also cannot reveal the velocity distribution in the vessel with high level accuracy. 4D MRI velocity scanning has received rapid development recently, so we can compare the simulation results with real flow conditions.

## Reference

- [1] M. F. Fillinger, M. L. Raghavan, S. P. Marra, J. L. Cronenwett, and F. E. Kennedy, "In vivo analysis of mechanical wall stress and abdominal aortic aneurysm rupture risk," *Journal of vascular surgery*, vol. 36, no. 3, pp. 589-597, 2002.
- [2] L. C. Brown and J. T. Powell, "Risk factors for aneurysm rupture in patients kept under ultrasound surveillance," *Annals of surgery*, vol. 230, no. 3, p. 289, 1999.
- [3] J. Cronenwett *et al.*, "Actuarial analysis of variables associated with rupture of small abdominal aortic aneurysms," *Surgery*, vol. 98, no. 3, pp. 472-483, 1985.
- [4] W. D. Clouse *et al.*, "Acute aortic dissection: population-based incidence compared with degenerative aortic aneurysm rupture," in *Mayo Clinic Proceedings*, 2004, vol. 79, no. 2, pp. 176-180: Elsevier.
- [5] S. Juvela, M. Porras, and K. Poussa, "Natural history of unruptured intracranial aneurysms: probability of and risk factors for aneurysm rupture," *Journal of neurosurgery*, vol. 93, no. 3, pp. 379-387, 2000.
- [6] Z. Kulcsár *et al.*, "Intra-aneurysmal thrombosis as a possible cause of delayed aneurysm rupture after flow-diversion treatment," *American Journal of Neuroradiology*, vol. 32, no. 1, pp. 20-25, 2011.
- [7] L. Waite and J. M. Fine, "Applied biofluid mechanics," 2007.
- [8] D. Liepsch, "An introduction to biofluid mechanics—basic models and applications," *Journal of biomechanics*, vol. 35, no. 4, pp. 415-435, 2002.
- [9] R. J. Cody *et al.*, "Atrial natriuretic factor in normal subjects and heart failure patients. Plasma levels and renal, hormonal, and hemodynamic responses to peptide infusion," *Journal of Clinical Investigation*, vol. 78, no. 5, p. 1362, 1986.
- [10] A. C. Burleson and V. T. Turitto, "Identification of quantifiable hemodynamic factors in the assessment of cerebral aneurysm behavior. On behalf of the Subcommittee on Biorheology of the Scientific and Standardization Committee of the ISTH," *Thrombosis and haemostasis*, vol. 76, no. 1, pp. 118-123, 1996.
- [11] G. Strang and G. J. Fix, *An analysis of the finite element method*. Prentice-hall Englewood Cliffs, NJ, 1973.
- [12] M. Castro, C. Putman, and J. Cebal, "Computational fluid dynamics modeling of intracranial aneurysms: effects of parent artery segmentation on intra-aneurysmal hemodynamics," *American Journal of Neuroradiology*, vol. 27, no. 8, pp. 1703-1709, 2006.
- [13] G. Dhatt, E. Lefrançois, and G. Touzot, *Finite element method*. John Wiley & Sons, 2012.
- [14] K.-J. Bathe and E. L. Wilson, "Numerical methods in finite element analysis," 1976.
- [15] W. R. Milnor, "Hemodynamics," 1982.
- [16] A. Böyum, "Isolation of mononuclear cells and granulocytes from human blood. Isolation of mononuclear cells by one centrifugation, and of granulocytes by combining centrifugation and sedimentation at 1 g," *Scandinavian journal of clinical and laboratory investigation. Supplementum*, vol. 97, pp. 77-89, 1967.
- [17] A. Karmen, F. Wróblewski, and J. S. LaDue, "Transaminase activity in human blood," *Journal of Clinical Investigation*, vol. 34, no. 1, p. 126, 1955.
- [18] F. Rengier *et al.*, "3D printing based on imaging data: review of medical applications," *International journal of computer assisted radiology and surgery*, vol. 5, no. 4, pp. 335-341, 2010.
- [19] D. Dimitrov, W. Van Wijck, K. Schreve, and N. De Beer, "Investigating the achievable accuracy of three dimensional printing," *Rapid Prototyping Journal*, vol. 12, no. 1, pp. 42-52, 2006.
- [20] A. Fluent, "12.0 Theory Guide," *Ansys Inc*, vol. 5, 2009.
- [21] C. Ansys, "Solver Theory Guide," *Ansys CFX Release*, vol. 11, pp. 1996-2006, 2006.
- [22] A. Fluent, "12.0 User's guide," *User Inputs for Porous Media*, vol. 6, 2009.
- [23] C. Ansys, "Ansys Inc," *Canonsburg, PA, USA*, 1998.
- [24] T. Stolarski, Y. Nakasone, and S. Yoshimoto, *Engineering analysis with ANSYS software*. Butterworth-Heinemann, 2011.

- [25] M. V. S. Sousa, E. C. Vasconcelos, G. Janson, D. Garib, and A. Pinzan, "Accuracy and reproducibility of 3-dimensional digital model measurements," *American journal of orthodontics and dentofacial orthopedics*, vol. 142, no. 2, pp. 269-273, 2012.
- [26] S.-M. Hu, Y.-F. Li, T. Ju, and X. Zhu, "Modifying the shape of NURBS surfaces with geometric constraints," *Computer-Aided Design*, vol. 33, no. 12, pp. 903-912, 2001.
- [27] R. Temam, *Navier-stokes equations*. North-Holland Amsterdam, 1984.
- [28] C. S. Peskin, "Numerical analysis of blood flow in the heart," *Journal of computational physics*, vol. 25, no. 3, pp. 220-252, 1977.
- [29] J. Bergendahl and D. Grasso, "Prediction of colloid detachment in a model porous media: hydrodynamics," *Chemical Engineering Science*, vol. 55, no. 9, pp. 1523-1532, 2000.
- [30] L. Formaggia, J.-F. Gerbeau, F. Nobile, and A. Quarteroni, "On the coupling of 3D and 1D Navier–Stokes equations for flow problems in compliant vessels," *Computer Methods in Applied Mechanics and Engineering*, vol. 191, no. 6, pp. 561-582, 2001.
- [31] L. Lee and R. J. LeVeque, "An immersed interface method for incompressible Navier–Stokes equations," *SIAM Journal on Scientific Computing*, vol. 25, no. 3, pp. 832-856, 2003.
- [32] C.-C. Lu, "A fast algorithm based on volume integral equation for analysis of arbitrarily shaped dielectric radomes," *IEEE Transactions on Antennas and Propagation*, vol. 51, no. 3, pp. 606-612, 2003.
- [33] W. B. Frakes and R. Baeza-Yates, "Information retrieval: data structures and algorithms," 1992.
- [34] T. Kersten and M. Lindstaedt, "Image-based low-cost systems for automatic 3D recording and modelling of archaeological finds and objects," *Progress in cultural heritage preservation*, pp. 1-10, 2012.